

# Methods for Assessing Mitochondrial Function in Diabetes

Christopher G.R. Perry,<sup>1</sup> Daniel A. Kane,<sup>2</sup> Ian R. Lanza,<sup>3</sup> and P. Darrell Neuffer<sup>4</sup>

A growing body of research is investigating the potential contribution of mitochondrial function to the etiology of type 2 diabetes. Numerous *in vitro*, *in situ*, and *in vivo* methodologies are available to examine various aspects of mitochondrial function, each requiring an understanding of their principles, advantages, and limitations. This review provides investigators with a critical overview of the strengths, limitations and critical experimental parameters to consider when selecting and conducting studies on mitochondrial function. *In vitro* (isolated mitochondria) and *in situ* (permeabilized cells/tissue) approaches provide direct access to the mitochondria, allowing for study of mitochondrial bioenergetics and redox function under defined substrate conditions. Several experimental parameters must be tightly controlled, including assay media, temperature, oxygen concentration, and in the case of permeabilized skeletal muscle, the contractile state of the fibers. Recently developed technology now offers the opportunity to measure oxygen consumption in intact cultured cells. Magnetic resonance spectroscopy provides the most direct way of assessing mitochondrial function *in vivo* with interpretations based on specific modeling approaches. The continuing rapid evolution of these technologies offers new and exciting opportunities for deciphering the potential role of mitochondrial function in the etiology and treatment of diabetes. *Diabetes* 62:1041–1053, 2013

**T**here has been a dramatic expansion in research investigating the role of mitochondria in the etiology of type 2 diabetes. This trend has been fueled, in part, by recent technological advances for assessing mitochondrial function. The advent of new tools and methodologies requires an understanding of the potential advantages and limitations of each. Unfortunately, relatively few consolidated resources are available to introduce methodologies for assessing mitochondrial bioenergetics—a field that focuses on direct and indirect measures of ATP synthesis as well as redox and ion homeostasis. While fundamentals of bioenergetics are covered elsewhere (1–3), the purpose of this review is to provide an introduction to the principles, advantages, and limitations to key methodologies used to study mitochondrial function *in vitro*, *in situ*, and *in vivo*. Our intent is

to assist in the selection of appropriate methodologies by highlighting relevant characteristics of major approaches, and to discuss recent issues in optimizing established methodologies.

## DEFINING AND MEASURING “MITOCHONDRIAL FUNCTION”

The synthesis of ATP via oxidative phosphorylation is the most common function ascribed to mitochondria. This process is typically determined indirectly through measurement of mitochondrial oxygen (O<sub>2</sub>) consumption, or respiration. Hence, altered respiratory kinetics in response to specific substrates are often interpreted as reflecting changes in oxidative phosphorylation and the regulation of cellular energy homeostasis *in vivo*. However, in addition to ATP synthesis, mitochondria play a central role in establishing and regulating cellular redox homeostasis. The present review provides an overview of the leading methods used to examine both of these functions.

**Respirometry.** In 1956, Chance and Williams (4) published the definitions of different respiratory steady-states based on the typical order of substrate additions made during an experiment on isolated mitochondria. These definitions have since been modified by Nicholls and Ferguson (2), reflecting an alternative sequence of substrate additions used during many mitochondrial experiments (Table 1). Under this system of nomenclature, state 1 refers to the O<sub>2</sub> consumption rate of mitochondria alone prior to addition of exogenous substrates or ADP. State 1 O<sub>2</sub> consumption rate is minimal. Addition of substrate(s) provides the fuel necessary to support the mitochondria, generating an increase in O<sub>2</sub> consumption (state 2) that largely reflects the basal rate of proton conductance (i.e., leak) back into the mitochondrial matrix. State 3 refers to the rate of respiration generated upon addition of ADP, and therefore exceeds state 2. State 4 refers to the rate of respiration remaining after all ADP has been converted to ATP. Although state 2 and state 4 respiration are empirically equivalent, state 4 is conventionally used when referring to respiration under basal, nonphosphorylating conditions. The respiratory control ratio, defined as the quotient of maximal state 3 to state 4 respiration, is often used as an index of mitochondrial coupling of oxidation (O<sub>2</sub> consumption) to phosphorylation of ADP to ATP, and thus the functional integrity of mitochondrial preparations. Familiarization with the development of these and other conventions are strongly recommended by referring to several key resources (1,2,4–9).

**Measuring mitochondrial respiration.** Measuring the rate of mitochondrial respirometric O<sub>2</sub> flux is accomplished by a number of methods, including O<sub>2</sub>-dependent quenching of porphyrin-based phosphors (10) and amperometric O<sub>2</sub> sensors (7). Although phosphorescent probes are growing in use for *in vitro/in situ* respiratory measurements (e.g., the Seahorse Bioscience XF Extracellular

From the <sup>1</sup>School of Kinesiology and Health Science, York University, Toronto, Ontario, Canada; the <sup>2</sup>Department of Human Kinetics, St. Francis Xavier University, Antigonish, Nova Scotia, Canada; the <sup>3</sup>Division of Endocrinology, Mayo Clinic College of Medicine, Rochester, Minnesota; and the <sup>4</sup>East Carolina Diabetes and Obesity Institute, Departments of Physiology and Kinesiology, East Carolina University, Greenville, North Carolina.

Corresponding author: Christopher G.R. Perry, [cperry@yorku.ca](mailto:cperry@yorku.ca).

Received 5 September 2012 and accepted 8 December 2012.

DOI: 10.2337/db12-1219

C.G.R.P. and D.A.K. contributed equally to this work.

The opinions expressed in this article are those of the authors and do not necessarily reflect the views of the National Institutes of Health.

© 2013 by the American Diabetes Association. Readers may use this article as long as the work is properly cited, the use is educational and not for profit, and the work is not altered. See <http://creativecommons.org/licenses/by-nc-nd/3.0/> for details.

See accompanying articles, pp. 1032 and 1036.

TABLE 1  
A comparison of the respiratory steady-state conventions

Author(s)	Respiration terminology	Relative O <sub>2</sub> flux	Characteristics
Chance and Williams (4)	State 1	Negligible	Mitochondria alone
	State 2	Negligible or low	ADP added, low/no substrate*
	State 3	High	ADP present, substrate added
	State 4	Low	Low ADP (converted to ATP), substrate present
	State 5	Negligible	Oxygen depleted from experimental chamber
Gnaiger (130)	LEAK	Low	Maximal substrate, no ADP
	OXPPOS	High	Maximal ADP and substrate
	ETS	Very high	Maximal substrate, uncoupler present

\*State 2 defined as “substrate present, ADP low” by Nicholls and Ferguson (2). ETS, electron transport system; LEAK, respiration due to basal proton conductance across the inner mitochondrial membrane; OXPPOS, oxidative phosphorylation.

Flux Analyzer or Luxcel MitoXpress) and are particularly useful for in vivo estimates of O<sub>2</sub> consumption in cultured cells (11), the amperometric approach has historically been the most common for in vitro investigations of mitochondrial respiration. The Clark electrode contains a gold or platinum cathode and an Ag/AgCl anode separated by a KCl solution. A voltage is applied to the two half-cells, which are separated from the experimental assay media by a membrane of O<sub>2</sub>-permeant material (e.g., polyvinylidene difluoride). O<sub>2</sub> diffuses from the assay media through the membrane and is reduced by electrons at the cathode, yielding hydrogen peroxide (H<sub>2</sub>O<sub>2</sub>). The H<sub>2</sub>O<sub>2</sub> then oxidizes the Ag of the Ag/AgCl anode, which generates an electrical current proportional to the partial pressure, and in turn concentration, of O<sub>2</sub> in the experimental solution (7). Changes in [O<sub>2</sub>] in the assay media (typically 1–2 mL) therefore correspond to the inverse of the respiratory rate of a biological sample (e.g., mitochondria) and allow for quantification of O<sub>2</sub> consumption (7).

The introduction of the XF Extracellular Flux Analyzer (Seahorse Bioscience) in 2006 represented a technical breakthrough for the field of bioenergetics by providing the first instrument with the capacity to measure in vivo O<sub>2</sub> consumption in intact adherent cells in culture. The system uses a 24- or 96-well cell culture microplate format that is mated from above with a sensor cartridge containing an equivalent number of individual probes, each containing fluorophores sensitive to O<sub>2</sub> or H<sup>+</sup> embedded within the polymer that comprises the probe. This piston-like sensor cartridge is introduced periodically into the wells of the microplate, forming transient microchambers just above (~200 microns) the cell monolayer. Fiber optic bundles inserted simultaneously by the machine into the probes of the sensor cartridge provide the excitation and collect the emission light for each fluorophore. The change in O<sub>2</sub> and H<sup>+</sup> concentration in the media (7–10 μL) is measured over several minutes, reflecting the rate of cellular O<sub>2</sub> consumption and H<sup>+</sup> production. Raising the sensor cartridge then allows the media above the cells to mix/reequilibrate. The XF Extracellular Flux Analyzer can also measure extracellular acidification rates and carbon dioxide evolution rates as indices of glycolysis and tricarboxylic acid cycle (TCA) kinetics.

**Technical considerations and limitations.** Accurate amperometric measurement of O<sub>2</sub> consumption is best achieved through high-resolution respirometric systems incorporating materials and structural designs that provide minimal O<sub>2</sub> leak and maximal sensitivity to O<sub>2</sub>. To this end, manufacturers of respirometric systems (e.g., OROBOROS

Instruments, Strathkelvin Instruments, Hansatech Instruments, etc.) incorporate 1) closed, air-tight reaction chambers; 2) glass and/or low O<sub>2</sub>-permeable polymers comprising all components (chamber seals, stir bars, etc), which minimizes O<sub>2</sub> back-diffusion and over-estimations of respiration; and 3) sensors capable of detecting changes in [O<sub>2</sub>] with minimal noise. High resolution designs (i.e., O2k, OROBOROS Instruments) maximize respirometric sensitivity and precision (minimal O<sub>2</sub> leak and highly sensitive electrodes), reducing the biological sample size required. Software advances in flux derivations of changes in chamber PO<sub>2</sub> also permit real-time reporting of respiratory kinetics (Datlab, OROBOROS Instruments), which improves data analyses over other systems requiring visual assessments of steady-state kinetics. Moreover, the unavoidable background O<sub>2</sub> consumption by the electrode itself, combined with varying degrees of O<sub>2</sub> back-diffusion into the oxygenic chamber, constitute potential sources of systematic error. In high-resolution systems, global instrumental background O<sub>2</sub> consumption (i.e., nonbiological O<sub>2</sub> flux), which increases positively as a function of PO<sub>2</sub>, must be corrected for accurate determinations of absolute O<sub>2</sub> consumption.

All amperometric-based approaches are suitable for studying isolated mitochondria, permeabilized cells/tissue and/or intact cells in suspension. Most provide injection ports and/or infusion systems for introducing substrates, reagents, and/or inhibitors without exposing the chamber solution to ambient O<sub>2</sub>. Units with peltier control of temperature permit comparisons of functional kinetics at precise temperatures, a critical parameter (see “Controlling critical experimental parameters: temperature”), but this is not available in all systems. In addition, the capability of the O2k system (OROBOROS Instruments) has recently expanded beyond respiration to permit simultaneous fluorescence-based measurements, potentiometric measurements of H<sup>+</sup> (i.e., pH), triphenylphosphonium (membrane potential probe), and Ca<sup>2+</sup>, as well as amperometric measurement of nitric oxide. High stirring capacities (i.e., several hundred rpm) in all closed systems prevent gradients from forming between the biological source in solution (i.e., isolated mitochondria, permeabilized tissue/cells, etc.) and the detector(s). Positioning the O<sub>2</sub> electrode at a 45° angle relative to the bottom of the chamber (e.g., O2k) also insures stirring about the electrode is optimized (7). Sample stirring also ensures maximal exposure of tissue surface area to the surrounding assay media, which is critical for optimizing diffusion of substrates and O<sub>2</sub> to sample cores. However,

as most cell culture-based studies are conducted on adherent cells, the utility of solution-based systems is obviously limited when the experimental objective is to assess cellular bioenergetics in intact cultured cells. The effect(s), per se, of rapid stirring on the function of either isolated mitochondria or permeabilized fibers and cells has not, to our knowledge, been systematically tested. However, it has been noted that with the gentle stirring involved in the preparation of saponin-permeabilized human skeletal muscle fibers, less than 4% of total citrate synthase is liberated in both the permeabilization and wash steps (12).

As described above, the XF Extracellular Flux Analyzer (Seahorse Bioscience) minimizes the potential limitation for adherent cells by transiently limiting the volume of solution in which  $O_2$  and  $H^+$  are measured to just above the monolayer of cultured cells. However, this temporary microenvironment is not completely isolated from atmospheric  $O_2$  because of the potential for exchange with the surrounding media (i.e., the piston-like sensor probes do not form a seal when lowered into the well) and the plastic comprising the microplate wells (i.e., polystyrene is permeable to  $O_2$  [13,14]). Consequently, as  $[O_2]$  declines in the chamber volume above the cells during longer measurement periods, a gradient is created favoring diffusion of  $O_2$  from the media surrounding the sensor probe and the walls of the well into the measurement volume. This counteracts declines in assay  $[O_2]$  due to respiration leading to an underestimation of cellular respiration rate. Likewise, in protocols in which anoxia is reached and the media is then reoxygenated by mixing, diffusion of  $O_2$  back into the depleted chamber from the chamber walls can lead to overestimation of low rates during the subsequent measurement period. This limitation has been addressed through the development of a compartment-model-based algorithm to account for both sources of  $O_2$  diffusion (15).

Aside from the obvious biological relevance of assessing bioenergetic function in intact cells, the XF Extracellular Flux Analyzer offers a much higher throughput platform than the traditional Clark electrode-based systems. This is advantageous for screening-based applications; e.g., screening drug candidates for potential mitochondrial toxicity. Since its introduction, the XF Extracellular Flux Analyzer has been validated for a variety of different cell types (16–20), including single muscle fibers (21). However, many substrates and compounds used to target specific mitochondrial pathways do not cross the cell membrane. Therefore, targeted probing of potential changes in mitochondrial function often requires gaining direct access to mitochondria, either via permeabilization or by isolating mitochondria. Because of their versatility and expanding capabilities, amperometric-based closed systems have historically been the method of choice for isolated mitochondria or permeabilized cells/tissue. However, if high throughput is needed, the XF Extracellular Flux Analyzer may be used by adhering mitochondria to the bottom of the microplate with a brief centrifugation step (19). No specific coating of the microplate is required, and the mitochondria remain attached through repeated mixing/measuring cycles. Care must be taken not to overload the wells, which can cause  $O_2$  to quickly become depleted under state 3 conditions. Substrates (e.g., ADP, etc.) may also become depleted from the small microchamber volume (7  $\mu$ L) and thus be rate limiting. Similar to the situation with  $O_2$ , although the chamber is semiopen, rates of substrate utilization by the plated mitochondria may exceed the diffusion capacity from the media surrounding the microchamber, necessitating the testing and use of higher

initial substrate concentrations than typically required in closed systems that are not limited by volume or diffusion (19). Use of permeabilized muscle fiber bundles has not been validated in the XF Extracellular Flux Analyzer.

**Oxidant emission.** Another key function of mitochondria is the regulation of cellular redox homeostasis through the establishment of the redox circuitry (e.g., via the NADPH/NADP couple) and emission of reactive oxidants. The redox circuitry extends throughout the proteome and represents a major mechanism of controlling multiple cell functions (22–24). This has particular relevance to the study of metabolic health given that oxidant emission (oxidant production minus oxidant scavenging) and redox signaling have been implicated in the etiology of insulin resistance in multiple tissues, including skeletal muscle (reviewed in 3,25–27).

Reactive  $O_2$  species (ROS) is an umbrella term used to describe molecules that are chemically reactive due to the incomplete reduction of  $O_2$  within the molecule. These include free radicals possessing an unpaired electron such as the superoxide anion ( $O_2^{\bullet -}$ ), hydroxyl radical ( $HO^{\bullet}$ ), peroxy and nitroxyl radicals, as well as nonradical oxidants such as  $H_2O_2$  (22). However, the term oxidants generally encompasses ROS, reactive nitrogen species, and reactive lipid species (26,28,29). Because of their relative instability, oxidants are generally quite difficult to study, a fact highlighted by the historical lack of widely available tools to measure oxidants (30). Electron spin resonance/electron paramagnetic resonance represents the most direct way to detect free radicals, an approach that can be used in vivo under physiological conditions (31,32). A variation on the technique, known as spin trapping, is also frequently used; it incorporates a detecting molecule that reacts with, but is considerably more stable than, the initial free radical. The resulting free radical product often has spectral properties that allow the original radical to be identified indirectly. Although clinical applications continue to develop (33), in general electron spin resonance/electron paramagnetic resonance spectroscopy is limited in both its specificity and sensitivity to quantitatively detect free radicals typically associated with biological systems (31,32). Furthermore, this method does not detect nonradical oxidants.

Several fluorescent, chemiluminescent, and, most recently, electrochemical/nanoparticle-based (34) approaches are available to detect oxidants. Fluorescent probes are arguably the most common method used to detect a variety of oxidants (35). For example, oxidation of the widely used 2',7'-dichlorodihydrofluorescein can give a sense of ROS burst. However, dichlorodihydrofluorescein is notorious for its relative lack of specificity and is subject to auto-oxidation and photo-oxidation (36). Mitochondrial  $O_2^{\bullet -}$ , the parent molecule of all ROS, can be detected fluorescently by the mitochondrial-targeted triphenylphosphonium hydroethidine-based probe MitoSOX Red (Invitrogen) (37). However, MitoSOX Red also reacts with other oxidant species to generate products with overlapping emission spectra, although this limitation can be overcome through use of an alternative detection system based on capillary electrophoresis (38,39). In biological systems however, mitochondrial  $O_2^{\bullet -}$  is rapidly and efficiently converted by manganese superoxide dismutase to  $H_2O_2$ , a membrane-permeable nonradical oxidant recognized for its role as a biological second messenger (22,30,40–42).

First described by Mohanty et al. (43), the redox-sensitive fluorogenic AmplexRed (*N*-acetyl-3,7-dihydroxyphenoxazine)

has become the most commonly used reagent for detecting  $H_2O_2$  in the past ten years. Unlike its predecessor scopoletin, AmplexRed (and the latest AmplexUltraRed) is a colorless and nonfluorescent derivative of dihydroresorufin, which is oxidized by  $H_2O_2$  via horseradish peroxidase (1:1 reaction stoichiometry) to the highly fluorescent resorufin (44). A number of ratiometric- as well as genetic-based fluorescent probes with high specificity for  $H_2O_2$  have recently been developed for use in living cells, including sensors that are targeted to various cellular locations (45–48). These tools provide unprecedented ability to visualize by confocal microscopy in real time the spatiotemporal nature of cellular  $H_2O_2$  production and its impact on local redox environments.

#### **Measuring mitochondrial oxidant emission potential.**

Measuring mitochondrial oxidant production has been accomplished using isolated mitochondria or permeabilized cells/tissue. The method is based on the general principle that the mitochondrial respiratory chain is a redox system reflecting the balance between the reducing potential of redox couples feeding into and through the system and the rate of proton conductance across the mitochondrial inner membrane into the matrix (2,3). Reducing potential within the electron transport system can be raised by increasing the supply and/or blocking the flow of electrons (e.g., with specific inhibitors), creating conditions that lead to electron leak and  $O_2 \cdot^-$  generation, and in turn  $H_2O_2$ .  $H_2O_2$  is uncharged and therefore freely diffuses out of the mitochondrial matrix, possibly facilitated by aquaporin channels (49), where it can be measured by one of the detection systems mentioned above. Various substrates in combination with inhibitors to specific sites within the respiratory complexes have been used to identify the sites and topology of  $O_2 \cdot^-$  production (50–52). It is important to recognize that both glutathione and thioredoxin provide significant  $H_2O_2$  scavenging capacity in the mitochondrial matrix (21,27); thus, the emission rate of  $H_2O_2$  from the mitochondria reflects the balance between  $H_2O_2$  production and scavenging rates and therefore underestimates the rate of  $O_2 \cdot^-$  production (44,45). Mitochondrial glutathione can be depleted by pretreatment with oxidizing agents such as 1-chloro-2,4-dinitrobenzene to obtain a more accurate measure of  $O_2 \cdot^-$  production (approximately twofold higher rate of  $H_2O_2$  emission by mitochondria) (53). It is important to note that measures of  $H_2O_2$  emission in permeabilized cells or isolated preparations are performed under substrate and respiratory conditions that are defined experimentally but do not and cannot perfectly replicate conditions in vivo. Thus, these represent estimates of the mitochondrial oxidant emitting potential (54) of the preparation under the experimental conditions chosen.

**Measurement of membrane potential.** Membrane potential across the inner membrane is a critical parameter in the study of overall mitochondrial function because it represents the balance between reduction potential of the proton pumps in the electron transport system and the rate of ion conductance (e.g.,  $H^+$ ) back across the membrane into the matrix. In essence, it reflects the redox state of the system and therefore the tendency of electrons to leak to  $O_2$  to form  $O_2 \cdot^-$ . A number of cationic fluorescent probes have been developed for assessing qualitative changes in mitochondrial membrane potential in cultured cells using both confocal microscopy and flow cytometry (55,56). Quantitative measures of membrane potential have typically been performed on isolated mitochondria using electrodes sensitive to potential-dependent probes such as

triphenylmethyl phosphonium cation (1,2). Calculation of membrane potential is based on the Nernst equation and requires an estimate of the matrix volume (per unit protein) over which the probe distributes.

**ATP production via bioluminescence.** ATP production rate has been used to provide an index of oxidative phosphorylation activity in isolated mitochondria. The ATP produced is detected through the reaction of luciferin with ATP to ultimately generate oxyluciferin, AMP, and light via firefly luciferase, which is detected in a luminometer (57). This method is typically performed on isolated mitochondria and provides a direct measure of ATP production rate rather than relying on the assumption that all ADP added is phosphorylated. This is particularly advantageous if a given experimental treatment may change coupling efficiencies (P/O ratios, reflecting the amount of ATP produced per  $O_2$  reduced to water during oxidative phosphorylation). Hence, a given respiration rate would no longer represent a specific rate of ATP production rendering conclusions regarding ATP synthesis quite difficult based on respiratory kinetics alone. A more detailed overview of this methodology is reviewed elsewhere (57).

**Calcium retention capacity.** The sensitivity of the permeability transition pore to calcium loading has been used as an index of mitochondrial viability and can be evaluated by determining the calcium retention capacity of mitochondria to Calcium Green-5N (Molecular Probes), a relatively low-affinity impermeable calcium indicator that exhibits an increase in fluorescence emission intensity upon binding calcium. Pulses of calcium are added at defined intervals, each eliciting a spike in signal that quickly dissipates due to the uptake of calcium into the mitochondrial matrix. Calcium concentration is monitored continuously with each addition until opening of the Permeability Transition Pore collapses the membrane potential and releases the accumulated calcium from the matrix, causing a sudden and sustained increase in signal. The amount of calcium retained prior to opening of the Permeability Transition Pore is considered an index of mitochondrial viability, particularly in the context of ischemia-reperfusion injury in the heart (58–60).

#### **SAMPLE PREPARATIONS: IN VITRO AND IN SITU APPROACHES**

**Isolated mitochondria.** Isolation of mitochondria through tissue/cell culture homogenization and differential centrifugation is routinely used for assessments of mitochondrial  $O_2$  consumption, oxidant emission, and membrane potential in a variety of tissues (1,61–65). This preparation is ideal for studying mitochondrial bioenergetics free from the influence of other cellular factors (e.g., cytoskeleton and endoplasmic reticulum). However, comparisons of isolated mitochondria to permeabilized muscle fiber bundles can be a powerful approach for isolating the effects of cytosolic structures in regulating mitochondrial function as highlighted previously (54,66–69). It also permits assessments of distinct subcellular pools of mitochondria, specifically subsarcolemmal and intermyofibrillar fractions of skeletal muscle, which appear to have unique functional properties (70). However, the disadvantages of the isolated mitochondria approach (described in ref. 62) include 1) disruption of mitochondrial structure, which may impact function, especially if fused into a continuous reticulum such as in mature skeletal muscle (62,69,71–75); 2) biased selection of certain mitochondrial populations in a given sample (e.g., less dense mitochondrial populations excluded from the

differential centrifugation step) (62,74); 3) requirement of relatively large sample sizes ( $>200 \cdot 10^6$  cells, or  $\geq 100$ – $150$  mg wet weight of tissue) to generate sufficient mitochondrial yields, which at best often amount to  $<20\%$  of the total population (61,62); and 4) loss of mitochondrial interactions with other cellular components, thus altering the functional properties (i.e., microcompartmentalization, metabolic channeling, and intracellular energy transfer) known to be present in vivo (62,76–79).

**Permeabilized tissue.** The scope within which mitochondrial functions can be analyzed in vivo is limited due to the fact that many exogenously added treatments (e.g., effectors such as ADP) do not readily penetrate cell membranes (62). Efforts to both circumvent the limitations associated with isolated mitochondrial preparations, and at the same time maintain the experimental freedoms conferred by the methodology, have led to established protocols involving chemically permeabilized cells (80). This method has also been adapted to assess mitochondria in multiple tissue types including cardiac muscle fibers (62,81), hepatocytes (82), adipose tissue (83,84), and especially skeletal muscle (62), although the application of this approach in each tissue requires careful consideration of unique limitations such as the ability to remove endogenous substrates following permeabilization. The successful permeabilization of cell membranes is achieved by cholesterol-specific detergents such as digitonin, filipin,  $\alpha$ -solanine,  $\alpha$ -tomatine, and  $\beta$ -escin (62). One of the most widely used permeabilizing agents is quillaja saponin, a relatively mild detergent (e.g., compared with digitonin [85]) derived from the soap bark tree (*Quillaja saponaria*) and referred to in the literature as simply saponin.

Saponins owe their detergent properties to hydrophilic glycoside moieties attached to lipophilic triterpene derivatives (86), which gives saponin its high affinity for cholesterol (62). Because plasma membranes contain approximately seven times more cholesterol ( $\sim 0.5$  mol cholesterol per mol phospholipid) than mitochondria (0.07 and 0.01 mol cholesterol per mol phospholipid for the mitochondrial outer and inner membranes, respectively) (87,88), very small concentrations of saponin (e.g., up to  $50 \mu\text{g} \cdot \text{mL}^{-1}$ ) are sufficient to selectively permeabilize the plasma membrane (62). Pores  $\sim 8$  nm in diameter are formed, providing an effective “washout” of soluble cytosolic contents and allowing direct access of exogenously added substrates/reagents to the mitochondria (89,90). Additional intracellular structures containing little or no cholesterol, such as the sarcoplasmic reticulum (SR) and the contractile apparatus will also remain intact upon saponin treatment (78). Furthermore, saponin concentrations as low as  $50 \mu\text{g} \cdot \text{mL}^{-1}$  have been shown to increase  $\text{Ca}^{+2}$  loss from the SR of mammalian cardiac and skeletal muscle (91,92) and to also reduce the ability of the SR to load  $\text{Ca}^{+2}$  (90). This is thought to result from the effect of saponin on the SR  $\text{Ca}^{+2}$  release channels, and not SR membrane permeabilization, per se (90). Because mitochondria are known to readily take up  $\text{Ca}^{+2}$  (93), the loss of  $\text{Ca}^{+2}$  from the SR during permeabilization is beneficial to studies involving mitochondrial function. Furthermore, normal mitochondrial morphology, including intact inner and outer mitochondrial membranes, has been verified by electron microscopy in saponin-permeabilized cardiac fibers due to a low abundance of cholesterol in these membranes (62,81). Mitochondrial integrity is often verified by adding exogenous cytochrome *c*, such that any additional increase in respiration is indicative of a disrupted

outer membrane (94). A common practice is to accept up to 10% increases in respiration upon addition of cytochrome *c* as evidence of preserved integrity, although this has yet to be validated. Indeed, it has been shown that isolated mitochondria can lose cytochrome *c* independent of outer membrane intactness (95). There is also evidence that a cytochrome *c* effect may depend on the substrates used to support respiration, although the reasons for this observation are not entirely clear (96,97). Moreover, it has been suggested that cytochrome *c* release into the cytosol in vivo is sufficient to maintain oxidative phosphorylation (96,98). In saponin-permeabilized cardiac fibers, the results of a cytochrome *c* test have even been noted to depend on the respiratory steady-state, with mitochondria in state 4 exhibiting greater cytochrome *c* responses than those in state 3 (97). There is an apparent paucity of studies in which the cytochrome *c* test is performed on isolated mitochondria, and those having reported the test results tend to indicate an increase in respiration after cytochrome *c* addition (99,100). Our own experience suggests that at  $37^\circ\text{C}$ , a cytochrome *c* response is unavoidable in mitochondria isolated from rat skeletal muscle using standard procedures (unpublished observations by D.A.K.). Thus, the cytochrome *c* test represents a convenient, but clearly imperfect means of testing for outer mitochondrial membrane intactness. When the objective is to establish the intactness of the mitochondria independent of the research hypothesis, the cytochrome *c* test should be performed during state 3 respiration.

When compared with isolated mitochondria, the advantages of the permeabilized fiber approach to study muscle mitochondria (described in 62) include 1) retention of the mitochondrial reticular morphology (66), 2) retention of potential interactions between mitochondria and other subcellular structures/organelles (cytoskeleton, contractile proteins, peroxisomes, endoplasmic reticulum, etc.) (67), and 3) small sample size (1–2 mg wet weight). Limitations include 1) the requirement for fresh tissue, although cryogenic freezing with glycerol-based media to prevent membrane rupturing has been reported (101)—but with limited effectiveness following long-term preservation (102); 2) the potential for diffusion limitations of  $\text{O}_2$  and substrates to the mitochondria; 3) the potential for nonmitochondrial-specific cationic probe distribution used in membrane potential measurements; 4) the propensity for permeabilized muscle fibers to contract in response to ADP (54,103); and 5) challenges in normalizing data to mitochondrial content. Regarding the latter, recent evidence suggests it may be possible to quantify mitochondria using protein densitometry in lyophilized samples postexperiment (104) or perhaps mitochondrial DNA or enzyme activities. However, the marker for mitochondrial content must be carefully considered, as not all markers have been shown to strongly correlate with total mitochondrial content (105). Furthermore, standard convention is to express functional data to wet weight, which is often recorded prior to an experiment, or dry weight, which requires retrieval of tissue sample from the reaction vessel. Dry weights avoid the inconsistencies in water contribution to total weight. However, blotting and weighing wet permeabilized muscle fibers prior to experimentation may affect certain respiratory metrics, particularly the apparent  $K_m$  to ADP ( $K_{mapp}$ ), which may be due to contraction in the absence of relaxing solution during weighing (unpublished observations by C.G.R.P. in rodent and human skeletal muscle). Certain tissues are prone to

disintegration during functional assessments in systems with stirring, although this is prevented by myosin ATPase inhibition in the case of skeletal muscle (54).

**Cultured cells.** Cultured cells provide several advantages, including the obvious relevance to *in vivo* biology, the ability to manipulate the expression of proteins of interest, and the ability to apply optical imaging of subcellular compartment-specific fluorophores targeted to specific proteins or biochemical signal generation. However, most immortalized cell lines are metabolically adapted for rapid growth, often require culture conditions that are nonphysiological (i.e., up to 25 mmol/L glucose), and derive most of their energy from glycolysis rather than mitochondrial oxidative phosphorylation (106,107). Primary cells in culture possess more physiologically relevant metabolic poise but are short lived and more technically challenging. Furthermore, care must be taken when interpreting O<sub>2</sub> consumption data, given that mitochondrial bioenergetics, regardless of the cell type used, is governed primarily by cellular energy demand.

#### CONTROLLING CRITICAL EXPERIMENTAL PARAMETERS

A number of experimental parameters can affect mitochondrial function and should be considered when designing experiments or clinical diagnostic tests. These include the composition of the respiration buffer, reaction temperature, O<sub>2</sub> concentration, and factors specific to working with permeabilized cells/tissues.

**Respiration buffer.** The goal of most *in vitro* or *in situ* studies is to replicate, as much as possible, the environment of mitochondria *in vivo*. To this end, assay media have been designed to control the concentration of specific ions and total osmolarity reflective of extracellular and intracellular conditions (Table 2). Isolated mitochondria are generally prepared in media rich in sucrose, a mitochondrial inner membrane-impermeant osmolyte, which is intended to promote stabilization of mitochondrial integrity (108,109). With permeabilized muscle fiber bundles, separation and permeabilization is achieved in the K<sup>+</sup>-based buffer (BIOPS [81]) or similar buffers with slight modifications (62,110). Respiration buffers are generally high K<sup>+</sup>-based media with physiological osmolarities

TABLE 2

Composition of preparation and respiration buffers for assessing mitochondrial respiratory kinetics in permeabilized muscle fiber bundles (all buffers) and isolated mitochondria (MiRO5)

	Buffer Z (ref. 54)	Mitomed (ref. 129)	MiRO5 (ref. 170)
EGTA	1 mmol/L	0.5 mmol/L	0.5 mmol/L
Taurine	0	20 mmol/L	20 mmol/L
Dithiothreitol	0	0.5 mmol/L	0
MgCl <sub>2</sub>	5 mmol/L	3 mmol/L	3 mmol/L
Sucrose	0	110 mmol/L	110 mmol/L
K-MES	105 mmol/L	0	0
KCl	30 mmol/L	0	0
K-lactobionate	0	60 mmol/L	60 mmol/L
KH <sub>2</sub> PO <sub>4</sub>	10 mmol/L	3 mmol/L	10 mmol/L
K-HEPES	0	20 mmol/L	20 mmol/L
Bovine serum			
albumin	5.0 mg/mL	2.0 mg/mL	1 mg/mL
Leupeptin	0	1 μmol/L	0
Soybean trypsin			
inhibitor	0	1 μmol/L	0
pH	7.1	7.1	7.1

(~295 mOsm) that differ largely with respect to sucrose and other stabilizing agents (54,62,110–112).

A special consideration of creatine and phosphocreatine (PCr) concentrations is required for the assessment of ADP-stimulated respiratory kinetics. Energy exchange (ADP/ATP) between matrix and cytosolic compartments can occur through creatine-dependent and -independent mechanisms. Optimal exchange is achieved by phosphate shuttling from matrix-derived ATP to creatine via mitochondrial creatine kinase in the intermembrane space with the PCr product then exported to the cytosol (113). This mechanism is depressed by PCr concentrations typical of relaxed skeletal muscle *in vivo* (54,114). In the absence of creatine, energy exchange is believed to occur less efficiently through direct ADP/ATP transport/diffusion across both mitochondrial membranes (66,113–117). The importance of supplementing assay media with creatine and PCr to control phosphate shuttling must therefore be considered when designing respirometric protocols.

**Temperature.** Historically, *in vitro* and *in situ* studies of mitochondrial function have typically been performed at 22–30°C for convenience and to maximize the duration of the experiment before O<sub>2</sub> becomes rate limiting. One might assume that respiratory fluxes measured at lower temperatures may be corrected to 37°C based on the Q<sub>10</sub> effect (respiration doubles for every 10°C increase). However, the respiratory system represents a balance between opposing forces (i.e., reducing potential of the electron transport system driving proton pumping versus the membrane potential across the inner membrane), and therefore the influence of temperature may not be as straightforward. Indeed, this problem has been addressed for biological systems in general (118). Data using permeabilized skeletal muscle fibers indicate that the actual temperature coefficients between respiration data obtained at 25°C or 30°C versus 37°C are much lower than 2, meaning decreasing temperature does tend to reduce respiration but the effect is much less than predicted (54). A Q<sub>10</sub> of less than 10 has also been reported in isolated mitochondria (119,120), which may suggest the diminished Q<sub>10</sub> effect relative to *in vitro* extraction-based determinations is due to properties within mitochondria rather than to mitochondrial morphology or the extramitochondrial environment that is largely retained in permeabilized muscle. In fact, increased stability of membranes and/or decreased ATPase activity have been suggested as potential factors to account for the lower rates of respiration at lower temperatures (121,122). Interestingly, isolated mitochondrial H<sub>2</sub>O<sub>2</sub> emission has been demonstrated to increase or decrease with temperature, depending on the species and tissue source (121,123). Thus, reaction temperature must be considered when designing experiments as the practical advantages of conducting experiments at lower temperature may compromise extrapolation of findings to physiological temperature.

**Permeabilized fiber bundles: contractile state.** Although not widely reported, permeabilized muscle fiber bundles tend to spontaneously contract, particularly in response to exogenous additions of ADP in a temperature-sensitive manner (54). This is potentially problematic as contraction may augment diffusion limitations for substrates and O<sub>2</sub>. Fortunately, contraction may be prevented through the use of nonspecific (e.g., pyrophosphate) (124,125) or specific (e.g., blebbistatin, *N*-benzyltoluene sulphonamide) (126,127) myosin ATPase inhibitors. In fact, direct comparison of respiratory kinetics in relaxed versus contracted fibers has revealed that contraction can

dramatically increase both the sensitivity (lower  $K_{mapp}$ ) and maximal responsiveness ( $V_{max}$ ) to ADP, depending on the muscle type and species (54,128). Disruptions in the interaction between the voltage-dependent anion channel, which participates in regulating ADP/ATP flux in and out of the mitochondria, with the cytoskeletal protein tubulin has recently been suggested as a mechanism by which contraction may alter mitochondrial ADP permeability (67). This is particularly intriguing, as it would represent a physical mechanism for increasing the sensitivity of the mitochondria to ADP at a time when it is most needed.

In the context of an experimental system however, exactly what causes permeabilized fibers to contract in the absence of added ADP/ATP is unresolved. Neither inhibition of potential cycling of residual endogenous ADP/ATP between creatine kinase and myosin-ATPase, nor limiting exposure to calcium (i.e., inclusion of high concentrations of the  $Ca^{2+}$ -chelator EGTA up to 5 mmol/L) prevents the spontaneous contraction (54), suggesting that the effect is independent of endogenous adenine nucleotide cycling or calcium. Treatment with trypsin induces a similar rapid shortening of permeabilized cardiomyocytes due to degradation of the cytoskeleton (68), leading Kuznetsov et al. (129) to raise the intriguing possibility that the presence of endogenous proteases may account for the apparent calcium-independent contraction in permeabilized muscle fibers. We recently tested this possibility in both rodent (Fig. 1) and human (115) permeabilized skeletal

muscle fiber bundles treated with protease inhibitors in three different respiration buffers, including Mitomed as recommended by Kuznetsov et al. (129). Inclusion of leupeptin, soybean trypsin inhibitor, and/or a protease inhibitor cocktail did not prevent contraction (see supplementary videos in ref. 115) nor the contraction-induced increase in respiratory sensitivity to ADP (i.e., lower  $K_{mapp}$ , Fig. 1). Thus, proteolytic degradation of the cytoskeleton does not appear to account for the spontaneous contraction. This leaves residual myosin-ATPase as the most likely explanation at this time (54), possibly related to rigor resulting from washout of ATP (103), although clearly further work is needed.

**Oxygen concentration.** It has been reported that  $O_2$  at air saturation ( $\sim 220 \mu\text{mol/L}$ ) rapidly becomes limiting to respiration in permeabilized muscle fibers due to diffusion limitations that are not present in cultured cells and isolated mitochondria in solution (130–132). This has prompted the practice of raising the initial  $O_2$  concentration in the respiration chamber to above air saturation (300–500  $\mu\text{mol/L}$ ) (133,134), which provides an additional benefit of avoiding frequent resupplementation of oxygen into the chamber during an experiment. A more recent study directly comparing air saturation ( $\sim 150\text{--}220 \mu\text{mol/L}$ ) with hyperoxia (275–450  $\mu\text{mol/L}$ ) failed to find any difference in maximal ADP-stimulated respiration in rodent red or white permeabilized muscle fiber bundles at 30°C or 37°C in high  $K^+$  respiration buffer (Buffer Z) (54). Surprisingly, the lack of

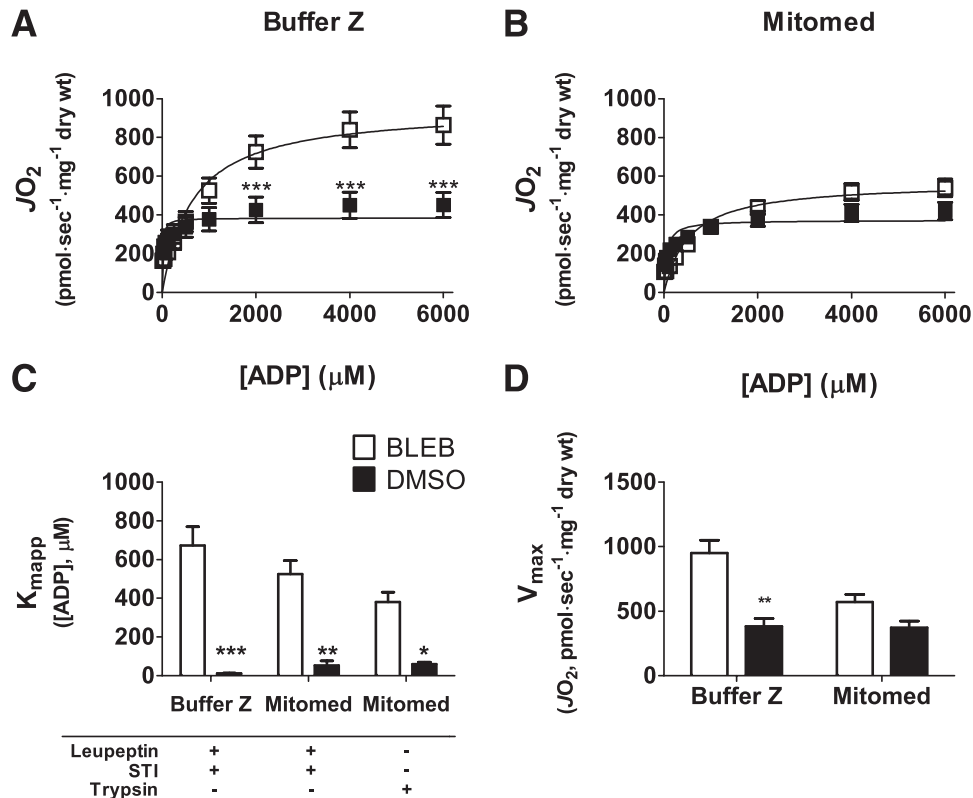


**FIG. 1.** The effect of protease inhibition or addition on contraction-mediated alterations in respiratory kinetics for ADP in Sprague-Dawley rat permeabilized red gastrocnemius fiber bundles. *A* and *B*: Michaelis-Menten-type line-fitting curves of respiratory  $O_2$  flux ( $JO_2$ ) in permeabilized muscle bundles, with 5 mmol/L pyruvate + 2 mmol/L malate, as a function of ADP concentration with the myosin II inhibitor blebbistatin (BLEB, 25  $\mu\text{mol/L}$ ), representing relaxed fibers, or vehicle (DMSO), representing contracted fibers, in two common respirometric assay media (Buffer Z [54,110,173] and Mitomed [129]). Protease inhibitors (1  $\mu\text{mol/L}$  leupeptin and soybean trypsin inhibitor [STI]) were included in wash and assay buffers. *C*: BLEB prevented the contraction-mediated (DMSO; spontaneous contraction) increase in respiratory sensitivity to ADP (i.e., lower  $K_{mapp}$ ) whether treated with protease inhibitors or protease (5  $\mu\text{mol/L}$  trypsin, 30 min in permeabilization buffer). *D*: The respiratory  $V_{max}$  in permeabilized muscle bundles was significantly greater with BLEB in Buffer Z only.  $n = 3$ , triplicate trials averaged. \*Significantly different than BLEB,  $P < 0.05$ ; \*\* $P < 0.01$ ; \*\*\* $P < 0.001$ .

effect of hyperoxia was independent of whether a contraction inhibitor was present or not (54). Similar data have been obtained in human permeabilized muscle fiber bundles (unpublished observation by C.G.R.P., D.A.K. and P.D.N.), suggesting that  $O_2$  concentrations above air saturation are not requisite for obtaining maximal  $O_2$  flux in permeabilized muscle under these experimental conditions. However, a significant impairment in  $K_{mapp}$  to ADP was reported with hyperoxia at 30°C, so care must still be taken when considering the assay  $O_2$  concentrations (54).

#### IN VIVO APPROACHES: NUCLEAR MAGNETIC RESONANCE

In most species, mitochondrial oxidative capacity is closely matched to maximal  $O_2$  consumption ( $VO_{2max}$ ) measured in vivo. Humans, however, are an interesting exception because mitochondrial respiratory capacity exceeds leg  $VO_2$  measured in vivo by arteriovenous  $O_2$  difference (135). This apparent discrepancy between mitochondrial  $VO_{2max}$  and muscle  $VO_{2max}$  was explained by limitations to  $O_2$  delivery to the contracting skeletal muscle (135). This unique aspect of human physiology has prompted careful scrutiny of methods to evaluate mitochondrial function in human skeletal muscle. As discussed previously, experiments in isolated mitochondria provide critical knowledge at the level of the intact organelle, whereas experiments in permeabilized muscle fibers are somewhat less reductionist by providing a window into the capacity and function of the entire population of mitochondria in the tissue. A well-recognized limitation of these in vitro methods is that measurements of  $O_2$  consumption are made in the absence of the circulatory system, a key limiter of  $VO_{2max}$  in humans. For many years, the Fick principle has been applied to measure leg  $VO_2$  from measurements of blood flow and arteriovenous  $O_2$  difference, but a variety of noninvasive methods have emerged more recently to evaluate mitochondrial capacity and function in skeletal muscle in vivo. This section of the review will provide a broad-strokes overview of several magnetic resonance-based approaches that are quickly becoming widespread in use.

**Oxidative capacity and basal ATP synthesis.** A common premise to each method is that a target tissue is positioned within a static magnetic field such as a clinical magnetic resonance imaging scanner. Within this magnetic field, certain atoms (e.g.,  $^1H$ ,  $^{13}C$ ,  $^{31}P$ ) resonate at unique frequencies when exposed to a second oscillating magnetic field. Nuclear magnetic resonance (NMR) spectroscopy and magnetic resonance spectroscopy (MRS) are one and the same, but the word “nuclear” is commonly dropped to avoid the common misconception that the procedure involves exposure to ionizing radiation. Phosphorous MRS ( $^{31}P$ -MRS) is a noninvasive technique that can be used to monitor the levels of high-energy phosphates (e.g., ATP, PCr) as well as other phosphorous-containing metabolites (inorganic phosphate [Pi], phosphomonoesters, and phosphodiester) in human skeletal muscle. A unique aspect of  $^{31}P$ -MRS in skeletal muscle is the high signal-to-noise, which permits rapid acquisition of spectra with temporal resolution of several seconds or less. Chance et al. (136) first applied  $^{31}P$ -MRS to investigate human skeletal muscle bioenergetics in the 1980s. Thirty years earlier, Chance and Williams (137) had established the regulatory role of ADP in controlling mitochondrial respiration. Chance applied the hyperbolic relationship between ADP and mitochondrial respiration to predict skeletal muscle

oxidative capacity from  $^{31}P$ -MRS measurements made during graded, progressive exercise (136). Owing to its micromolar concentration and bound state, it is not currently possible to directly measure free ADP using  $^{31}P$ -MRS in human muscle, but it can be calculated from the concentrations of other measureable metabolites using formulas described elsewhere (138). Chance showed that mitochondrial oxidative capacity could be predicted in vivo from a “transfer function” demonstrating a Michaelis-Menten-type relationship between progressive work (or the rate of respiration) and inorganic phosphate/PCr (ADP) (139). A major challenge of this approach is accurate measurement of muscle work and the critical assumption that the workloads are truly steady state.

A simpler method involves predicting skeletal muscle oxidative capacity using the kinetics of PCr recovery following a brief bout of muscle activity. During intense muscle contractions, the creatine kinase reaction buffers intracellular ATP levels at the expense of PCr, which falls rapidly. During a recovery period after exercise, PCr is resynthesized, and this repletion of PCr is a function of mitochondrial ATP synthesis. Since the ATP generated during recovery is driven primarily by oxidative metabolism, the rate of PCr recovery is a commonly used indicator of oxidative capacity (140–144). The assumption that PCr resynthesis is a function of mitochondrial ATP synthesis is supported by observations that PCr resynthesis is absent when the muscle is kept ischemic following muscle contraction, and PCr recovery occurs only upon reperfusion of the limb (145). More recent studies have shown some transient PCr resynthesis during ischemic recovery following muscle activity (146–148), owing to the ever-improving signal-to-noise and temporal resolution as magnetic resonance technology progresses. Notwithstanding, the transient glycolytic contribution to PCr resynthesis exerts minimal influence on the rate constant that defines PCr resynthesis over a 10-min recovery period. It is important to note that during the recovery period after exercise, the mitochondria are not working at their oxidative capacity; rather, oxidative capacity can be predicted from the rate at which PCr is regenerated. This approach has been shown to be highly reproducible (149–152) and well correlated with in vitro methods for assessing mitochondrial capacity (149,153,154). An advantage of this approach compared with the transfer function is that accurate measurement of muscle work is not necessary, but major assumptions are that ATP concentrations are stable and glycolytic flux is negligible during recovery.

Various approaches have been used to deplete PCr in skeletal muscle, ranging from resting ischemia (155), supramaximal stimulation of motor nerves (144), dynamic voluntary contractions (151), submaximal isometric contractions (150,153), and maximal voluntary contractions (140,149). Transcutaneous nerve stimulation is an attractive approach because the muscle can be maximally activated in a way that overcomes potential limitations in voluntary drive from higher centers. However, supramaximal motor nerve stimulation may not be well tolerated by all patient populations and poses a new set of challenges related to noise injection from the stimulator/electromyography cables breaching the shielded magnet room. Alternatively, maximal voluntary contractions can be performed by most patient populations. With sufficient habituation and visual feedback provided by a computer monitor or series of light-emitting diodes, it is possible to maximally activate skeletal muscles with no limitations of central motor drive (assessed



by superimposing electrical stimulation) (141). Although submaximal contractions are sometimes used to deplete PCr, the calculated oxidative capacity appears to be consistently lower compared with maximal contractions (150,151). The lower values derived from submaximal efforts may result from incomplete motor unit recruitment if the contraction intensity is below the threshold for complete motor unit recruitment. It is also possible that motor unit cycling during submaximal efforts could result in recruitment of new motor units as the muscle begins to fatigue while some initially recruited motor units no longer contribute to force production. Either case is problematic from the standpoint of measuring  $^{31}\text{P}$  metabolite levels by MRS. A phosphorous spectrum represents the average signal of all of the tissue within the sampling volume of the radiofrequency coil, regardless of whether the muscle is active or not. Therefore, the changes in  $^{31}\text{P}$  metabolites in the active muscle will be essentially "diluted" by the inactive tissue. Although this issue can be avoided by using supra-maximal stimulation or maximal voluntary contractions, one drawback is that PCr recovery is influenced by intramuscular pH. Careful attention is needed to ensure that the muscle contraction is sufficient to deplete PCr without acidosis by optimizing the duration of the exercise. Alternatively, it is possible to model mitochondrial capacity from the recovery rate of the calculated free ADP, which is independent of pH (150,156). In sum, the kinetics of PCr (or ADP) recovery following exercise is a reproducible, valid method to non-invasively evaluate skeletal muscle oxidative capacity. This approach, however, is restricted to skeletal muscle and cannot be used to evaluate mitochondrial capacity in other tissues such as liver, adipose, or brain.

In addition to measuring oxidative capacity,  $^{31}\text{P}$ -MRS can be used to measure basal ATP synthesis rates using magnetization-transfer techniques. The basic premise of this approach is that it is possible to calculate metabolic fluxes by perturbing the signal from a specific metabolite (e.g., ATP) and monitoring how this perturbation is transferred to another metabolite (e.g., Pi, PCr) that is linked by an exchange reaction (e.g.,  $\text{F}_1\text{F}_0$  ATPase, creatine kinase). An advantage over the PCr recovery approach is that magnetization transfer methods are not restricted to skeletal muscle tissues. There are several recent reviews that provide excellent detail on the principles and practice of this approach (157,158). An important point of emphasis is that metabolic fluxes measured by magnetization transfer are restricted to the steady-state conditions of resting muscle and cannot be used to evaluate mitochondrial oxidative capacity. Although the magnetization approach has been widely used to evaluate mitochondrial function (159–164), there continues to be lingering controversy over some aspects of the data and its interpretation (158). The main point of concern is that resting  $\text{Pi}\rightarrow\text{ATP}$  flux measured by  $^{31}\text{P}$ -MRS is  $\sim 10$ -fold higher than all other noninvasive measures of resting oxidative ATP synthesis. As pointed out by Kemp and Brindle (158), the exchange between Pi and ATP at rest is dominated by glycolytic enzymes (glyceraldehyde-3-phosphate dehydrogenase, phosphoglycerate kinase) and should not be interpreted as an index of mitochondrial ATP synthesis. Others contend that the glycolytic contribution is minimal at rest (165), and that the  $\text{Pi}\rightarrow\text{ATP}$  exchange scales as expected in mouse models in which mitochondrial protein abundance is genetically altered (166,167). The interested reader is pointed to several recent articles in which these considerations are extensively reviewed (157,158,168,169).

**Mitochondrial coupling.** The functionality of mitochondria is often inferred from their capacity to consume  $\text{O}_2$  or generate chemical energy. However, another important aspect of mitochondrial physiology is the efficiency of ATP synthesis by the organelles (i.e., coupling). Various approaches have been used to evaluate bioenergetic efficiency of isolated mitochondria (170) and in human skeletal muscle in vivo (171,172). This section of the review will touch briefly on two distinct in vivo approaches that have been applied to human skeletal muscle. The first approach combines optical spectroscopy and MRS to simultaneously measure  $\text{O}_2$  consumption and ATP production, respectively (155,171). The basic premise of this approach is to determine the P/O by quantifying both processes in parallel. Mitochondrial ATP synthesis is determined from the decline in PCr concentrations in resting ischemic muscle by  $^{31}\text{P}$ -MRS. During ischemia, mitochondrial ATP synthesis is suppressed and glycolytic ATP flux is minimal ( $<8\%$ ) (155,171). In the absence of aerobic or glycolytic ATP synthesis, intracellular PCr stores are consumed at a rate that reflects the ATP demand of the muscle. Mitochondrial ATP flux is determined using an ATP balance approach that assumes equality between ATP demand and mitochondrial ATP supply in resting muscle. Other assumptions include that ischemia does not change ATP demand, that glycolytic flux is negligible in resting muscle, and that ischemia does not alter glycolytic flux (155,171). Simultaneously,  $\text{O}_2$  consumption is measured in vivo by near infrared spectroscopy during the first minute of ischemia. A partial least squares analysis is used to differentiate between hemoglobin and myoglobin desaturation during ischemia. From these independent pieces of data acquired during ischemia, it is possible to determine the ratio of net ATP turnover to  $\text{O}_2$  uptake as a measure of mitochondrial bioenergetic efficiency. Although the  $^{31}\text{P}$ -MRS component is relatively straightforward, the measurement of  $\text{O}_2$  uptake requires substantial technical expertise, in vitro calibration sets, wavelength shift analysis to determine the ratio of different chromophores, and ability to measure deoxymyoglobin by proton MRS.

Another noninvasive NMR technique to evaluate bioenergetic efficiency of mitochondria involves measuring basal ATP flux by magnetization transfer paired with TCA flux measured by  $^{13}\text{C}$ -MRS (157,168,172). This approach deviates somewhat from the conventional definition of mitochondrial coupling at the level of the cytochrome chain; rather, it assesses efficiency from the ratio of substrate oxidation in the TCA to ATP synthesis. Assessment of TCA flux is made by infusing a magnetic resonance-visible tracer,  $[2\text{-}^{13}\text{C}]$  acetate, which enters the TCA after it is converted to acetyl CoA. Although the TCA intermediates are not present in sufficiently high concentrations to be directly measured by  $^{13}\text{C}$ -MRS, it is possible to monitor the time course of  $^{13}\text{C}$  enrichment of glutamate, which exchanges rapidly with  $\alpha$ -ketoglutarate. At this point, sophisticated modeling is required to determine the metabolic fate of the labeled acetate molecule. The details of this modeling are beyond the scope of this review, but are nicely detailed elsewhere (157,168,172). By pairing TCA flux with basal ATP synthesis measured by  $^{31}\text{P}$ -MRS magnetization transfer, it is possible to evaluate the efficiency of mitochondria, by comparing the level of substrate oxidation at a given level of basal ATP flux. Similar to the P/O measurements described above, this approach also requires substantial technical expertise, mathematical modeling, and careful attention to assumptions. It is important to note that

this estimate of mitochondrial efficiency differs from the more traditional direct measurements of phosphorylation efficiency measured *in vitro* by high-resolution respirometry or *in vivo* by the combination of optical spectroscopy and  $^{31}\text{P}$ -MRS described above. Nevertheless, all of the approaches described here represent theoretically plausible methods to evaluate aspects of mitochondrial coupling or efficiency, but as with any method, careful attention must be given to underlying critical assumptions.

## PERSPECTIVES AND CONCLUSIONS

To summarize, it is clear that a variety of experimental parameters and/or modeling approaches must be carefully considered in the context of the specific hypothesis being tested. Each method provides a unique set of advantages as well as limitations. The purest way to assess mitochondrial function free from other factors is to isolate mitochondria from the local environment, but this requires extensive disruption of mitochondrial structure and morphology with considerable loss of sample. Mitochondrial structure can be largely retained through simple chemical permeabilization of cell membranes providing access to mitochondrial compartments free from soluble cytoplasmic factors. However, numerous experimental parameters must be carefully controlled, and classic approaches for assessing certain bioenergetic parameters in isolated mitochondria (e.g., membrane potential) have not been fully developed in permeabilized tissue. Interestingly, combining multiple approaches may yield significant insight into the regulation of mitochondrial bioenergetics. For example, comparing the function of isolated mitochondria versus permeabilized samples is a powerful approach to determine the role of mitochondrial morphology or local structures in regulating mitochondrial function. Recent technological advances now permit assessment of respiratory control in intact adherent cultured cells, offering the opportunity for high through-put analyses in this specific model. Lastly, NMR is the most direct method for assessing mitochondrial function *in vivo*, especially in humans. Mathematical models have specifically targeted energetic components of mitochondrial function, with a focus on oxidative capacity, basal ATP synthesis, and coupling, which can be measured in real time. Ongoing developments in algorithms and conceptual assumptions have enhanced the power of this approach. The rapid progress of these technologies and approaches has expanded opportunities to investigate the potential contribution of mitochondrial bioenergetics and redox systems biology to the etiology of type 2 diabetes.

## ACKNOWLEDGMENTS

I.R.L. is supported by Clinical and Translational Science Award grant KL2 TR000136 from the National Center for Advancing Translational Science. P.D.N. is supported by grants from the National Institutes of Health (R01-DK074825 and R01-DK096907).

No potential conflicts of interest relevant to this article were reported.

C.G.R.P., D.A.K., I.R.L., and P.D.N. drafted parts of the text and edited the final manuscript. D.A.K. and P.D.N. contributed novel supporting data.

## REFERENCES

- Brand MD, Nicholls DG. Assessing mitochondrial dysfunction in cells. *Biochem J* 2011;435:297–312

- Nicholls DG, Ferguson SJ. *Bioenergetics 3*. San Diego, Academic Press, 2002
- Fisher-Wellman KH, Neuffer PD. Linking mitochondrial bioenergetics to insulin resistance via redox biology. *Trends Endocrinol Metab* 2012;23:142–153
- Chance B, Williams GR. The respiratory chain and oxidative phosphorylation. *Adv Enzymol Relat Subj Biochem* 1956;17:65–134
- Chance B, Williams GR. Respiratory enzymes in oxidative phosphorylation. III. The steady state. *J Biol Chem* 1955;217:409–427
- Gnaiger E. *Mitochondrial Pathways and Respiratory Control*. Innsbruck, OROBOROS MiPNet Publications, 2007
- Gnaiger E. Polarographic oxygen sensors, the oxygraph, and high-resolution respirometry to assess mitochondrial function. In *Drug-Induced Mitochondrial Dysfunction*. Dykens J, Will Y, Eds., Hoboken, John Wiley & Sons, Inc., 2008, p. 327–352
- Rasmussen HN, Rasmussen UF. Small scale preparation of skeletal muscle mitochondria, criteria of integrity, and assays with reference to tissue function. *Mol Cell Biochem* 1997;174:55–60
- Szendroedi J, Phielix E, Roden M. The role of mitochondria in insulin resistance and type 2 diabetes mellitus. *Nat Rev Endocrinol* 2011;8:92–103
- Wilson DF, Vinogradov S, Lo LW, Huang L. Oxygen dependent quenching of phosphorescence: a status report. *Adv Exp Med Biol* 1996;388:101–107
- Wu M, Neilson A, Swift AL, et al. Multiparameter metabolic analysis reveals a close link between attenuated mitochondrial bioenergetic function and enhanced glycolysis dependency in human tumor cells. *Am J Physiol Cell Physiol* 2007;292:C125–C136
- Tonkonogi M, Harris B, Sahlin K. Mitochondrial oxidative function in human saponin-skinned muscle fibres: effects of prolonged exercise. *J Physiol* 1998;510:279–286
- Wang B, Ogilby PR. Activation barriers for oxygen: diffusion in polystyrene and polycarbonate glasses: effects of codissolved argon, helium, and nitrogen. *Can J Chem* 1995;73:1831–1840
- Poulsen L, Zebger I, Tofte P, Klinger M, Hassager O, Ogilby PR. Oxygen diffusion in bilayer polymer films. *J Phys Chem B* 2003;107:13885–13891
- Gerencser AA, Neilson A, Choi SW, et al. Quantitative microplate-based respirometry with correction for oxygen diffusion. *Anal Chem* 2009;81:6868–6878
- Zhang J, Nuebel E, Wisidagama DR, et al. Measuring energy metabolism in cultured cells, including human pluripotent stem cells and differentiated cells. *Nat Protoc* 2012;7:1068–1085
- Maloyan A, Mele J, Muralimanohara B, Myatt L. Measurement of mitochondrial respiration in trophoblast culture. *Placenta* 2012;33:456–458
- Clerc P, Polster BM. Investigation of mitochondrial dysfunction by sequential microplate-based respiration measurements from intact and permeabilized neurons. *PLoS ONE* 2012;7:e34465
- Rogers GW, Brand MD, Petrosyan S, et al. High throughput microplate respiratory measurements using minimal quantities of isolated mitochondria. *PLoS ONE* 2011;6:e21746
- Schuh RA, Clerc P, Hwang H, et al. Adaptation of microplate-based respirometry for hippocampal slices and analysis of respiratory capacity. *J Neurosci Res* 2011;89:1979–1988
- Schuh RA, Jackson KC, Khairallah RJ, Ward CW, Spangenburg EE. Measuring mitochondrial respiration in intact single muscle fibers. *Am J Physiol Regul Integr Comp Physiol* 2012;302:R712–R719
- Jones DP. Radical-free biology of oxidative stress. *Am J Physiol Cell Physiol* 2008;295:C849–C868
- Ghezzi P, Bonetto V, Fratelli M. Thiol-disulfide balance: from the concept of oxidative stress to that of redox regulation. *Antioxid Redox Signal* 2005;7:964–972
- Brigelius-Flohé R. Commentary: oxidative stress reconsidered. *Genes Nutr* 2009;4:161–163
- Pérez-Matute P, Zulet MA, Martínez JA. Reactive species and diabetes: counteracting oxidative stress to improve health. *Curr Opin Pharmacol* 2009;9:771–779
- Bashan N, Kovsan J, Kachko I, Ovadia H, Rudich A. Positive and negative regulation of insulin signaling by reactive oxygen and nitrogen species. *Physiol Rev* 2009;89:27–71
- Muoio DM, Neuffer PD. Lipid-induced mitochondrial stress and insulin action in muscle. *Cell Metab* 2012;15:595–605
- Higdon A, Diers AR, Oh JY, Landar A, Darley-Usmar VM. Cell signalling by reactive lipid species: new concepts and molecular mechanisms. *Biochem J* 2012;442:453–464
- Kemp M, Go YM, Jones DP. Nonequilibrium thermodynamics of thiol/disulfide redox systems: a perspective on redox systems biology. *Free Radic Biol Med* 2008;44:921–937

30. Stone JR, Yang S. Hydrogen peroxide: a signaling messenger. *Antioxid Redox Signal* 2006;8:243–270
31. Sachdev S, Davies KJ. Production, detection, and adaptive responses to free radicals in exercise. *Free Radic Biol Med* 2008;44:215–223
32. Swartz HM, Khan N, Khrantsov VV. Use of electron paramagnetic resonance spectroscopy to evaluate the redox state in vivo. *Antioxid Redox Signal* 2007;9:1757–1771
33. Spasojević I. Free radicals and antioxidants at a glance using EPR spectroscopy. *Crit Rev Clin Lab Sci* 2011;48:114–142
34. Santhosh P, Manesh KM, Lee SH, Uthayakumar S, Gopalan AI, Lee KP. Sensitive electrochemical detection of superoxide anion using gold nanoparticles distributed poly(methyl methacrylate)-polyaniline core-shell electrospun composite electrode. *Analyst (Lond)* 2011;136:1557–1561
35. Kalyanaraman B, Darley-Usmar V, Davies KJ, et al. Measuring reactive oxygen and nitrogen species with fluorescent probes: challenges and limitations. *Free Radic Biol Med* 2012;52:1–6
36. Miller EW, Tulyathan O, Isacoff EY, Chang CJ. Molecular imaging of hydrogen peroxide produced for cell signaling. *Nat Chem Biol* 2007;3:263–267
37. Robinson KM, Janes MS, Pehar M, et al. Selective fluorescent imaging of superoxide in vivo using ethidium-based probes. *Proc Natl Acad Sci USA* 2006;103:15038–15043
38. Xu X, Arriaga EA. Qualitative determination of superoxide release at both sides of the mitochondrial inner membrane by capillary electrophoretic analysis of the oxidation products of triphenylphosphonium hydroethidine. *Free Radic Biol Med* 2009;46:905–913
39. Xu X, Thompson LV, Navratil M, Arriaga EA. Analysis of superoxide production in single skeletal muscle fibers. *Anal Chem* 2010;82:4570–4576
40. Rhee SG. Cell signaling.  $H_2O_2$ , a necessary evil for cell signaling. *Science* 2006;312:1882–1883
41. D'Auréaux B, Toledano MB. ROS as signalling molecules: mechanisms that generate specificity in ROS homeostasis. *Nat Rev Mol Cell Biol* 2007;8:813–824
42. Janssen-Heininger YM, Mossman BT, Heintz NH, et al. Redox-based regulation of signal transduction: principles, pitfalls, and promises. *Free Radic Biol Med* 2008;45:1–17
43. Mohanty JG, Jaffe JS, Schulman ES, Raible DG. A highly sensitive fluorescent micro-assay of  $H_2O_2$  release from activated human leukocytes using a dihydroxyphenoxazine derivative. *J Immunol Methods* 1997;202:133–141
44. Zhou M, Divu Z, Panchuk-Voloshina N, Haugland RP. A stable non-fluorescent derivative of resorufin for the fluorometric determination of trace hydrogen peroxide: applications in detecting the activity of phagocyte NADPH oxidase and other oxidases. *Anal Biochem* 1997;253:162–168
45. Dickinson BC, Huynh C, Chang CJ. A palette of fluorescent probes with varying emission colors for imaging hydrogen peroxide signaling in living cells. *J Am Chem Soc* 2010;132:5906–5915
46. Dickinson BC, Srikun D, Chang CJ. Mitochondrial-targeted fluorescent probes for reactive oxygen species. *Curr Opin Chem Biol* 2010;14:50–56
47. Fomenko DE, Koc A, Agisheva N, et al. Thiol peroxidases mediate specific genome-wide regulation of gene expression in response to hydrogen peroxide. *Proc Natl Acad Sci USA* 2011;108:2729–2734
48. Meyer AJ, Dick TP. Fluorescent protein-based redox probes. *Antioxid Redox Signal* 2010;13:621–650
49. Miller EW, Dickinson BC, Chang CJ. Aquaporin-3 mediates hydrogen peroxide uptake to regulate downstream intracellular signaling. *Proc Natl Acad Sci USA* 2010;107:15681–15686
50. Anderson EJ, Neuffer PD. Type II skeletal myofibers possess unique properties that potentiate mitochondrial  $H_2O_2$  generation. *Am J Physiol Cell Physiol* 2006;290:C844–C851
51. St-Pierre J, Buckingham JA, Roebuck SJ, Brand MD. Topology of superoxide production from different sites in the mitochondrial electron transport chain. *J Biol Chem* 2002;277:44784–44790
52. Muller FL, Liu Y, Van Remmen H. Complex III releases superoxide to both sides of the inner mitochondrial membrane. *J Biol Chem* 2004;279:49064–49073
53. Treberg JR, Quinlan CL, Brand MD. Hydrogen peroxide efflux from muscle mitochondria underestimates matrix superoxide production—a correction using glutathione depletion. *FEBS J* 2010;277:2766–2778
54. Perry CG, Kane DA, Lin CT, et al. Inhibiting myosin-ATPase reveals a dynamic range of mitochondrial respiratory control in skeletal muscle. *Biochem J* 2011;437:215–222
55. Cottet-Rousselle C, Ronot X, Leverve X, Mayol JF. Cytometric assessment of mitochondria using fluorescent probes. *Cytometry A* 2011;79:405–425
56. Perry SW, Norman JP, Barbieri J, Brown EB, Gelbard HA. Mitochondrial membrane potential probes and the proton gradient: a practical usage guide. *Biotechniques* 2011;50:98–115
57. Lanza IR, Nair KS. Functional assessment of isolated mitochondria in vitro. *Methods Enzymol* 2009;457:349–372
58. Heusch G, Boengler K, Schulz R. Inhibition of mitochondrial permeability transition pore opening: the Holy Grail of cardioprotection. *Basic Res Cardiol* 2010;105:151–154
59. Sloan RC, Moukdar F, Frasier CR, et al. Mitochondrial permeability transition in the diabetic heart: contributions of thiol redox state and mitochondrial calcium to augmented reperfusion injury. *J Mol Cell Cardiol* 2012;52:1009–1018
60. Di Lisa F, Carpi A, Giorgio V, Bernardi P. The mitochondrial permeability transition pore and cyclophilin D in cardioprotection. *Biochim Biophys Acta* 2011;1813:1316–1322
61. Frezza C, Cipolat S, Scorrano L. Organelle isolation: functional mitochondria from mouse liver, muscle and cultured fibroblasts. *Nat Protoc* 2007;2:287–295
62. Kuznetsov AV, Veksler V, Gellerich FN, Saks V, Margreiter R, Kunz WS. Analysis of mitochondrial function in situ in permeabilized muscle fibers, tissues and cells. *Nat Protoc* 2008;3:965–976
63. Picard M, Taivassalo T, Gousspillou G, Hepple RT. Mitochondria: isolation, structure and function. *J Physiol* 2011;589:4413–4421
64. Picard M, Hepple RT, Burelle Y. Mitochondrial functional specialization in glycolytic and oxidative muscle fibers: tailoring the organelle for optimal function. *Am J Physiol Cell Physiol* 2012;302:C629–C641
65. Lever JD, Chappell JB. Mitochondria isolated from rat brown adipose tissue and liver. *J Biophys Biochem Cytol* 1958;4:287–290
66. Kuznetsov AV, Tiivel T, Sikk P, et al. Striking differences between the kinetics of regulation of respiration by ADP in slow-twitch and fast-twitch muscles in vivo. *Eur J Biochem* 1996;241:909–915
67. Rostovtseva TK, Sheldon KL, Hassanzadeh E, et al. Tubulin binding blocks mitochondrial voltage-dependent anion channel and regulates respiration. *Proc Natl Acad Sci USA* 2008;105:18746–18751
68. Anmann T, Guzun R, Beraud N, et al. Different kinetics of the regulation of respiration in permeabilized cardiomyocytes and in HL-1 cardiac cells. Importance of cell structure/organization for respiration regulation. *Biochim Biophys Acta* 2006;1757:1597–1606
69. Picard M, Taivassalo T, Ritchie D, et al. Mitochondrial structure and function are disrupted by standard isolation methods. *PLoS ONE* 2011;6:e18317
70. Palmer JW, Tandler B, Hoppel CL. Biochemical properties of subsarcolemmal and interfibrillar mitochondria isolated from rat cardiac muscle. *J Biol Chem* 1977;252:8731–8739
71. Ogata T, Yamasaki Y. Ultra-high-resolution scanning electron microscopy of mitochondria and sarcoplasmic reticulum arrangement in human red, white, and intermediate muscle fibers. *Anat Rec* 1997;248:214–223
72. Kirkwood SP, Munn EA, Brooks GA. Mitochondrial reticulum in limb skeletal muscle. *Am J Physiol* 1986;251:C395–C402
73. Bach D, Pich S, Soriano FX, et al. Mitofusin-2 determines mitochondrial network architecture and mitochondrial metabolism. A novel regulatory mechanism altered in obesity. *J Biol Chem* 2003;278:17190–17197
74. Piper HM, Sezer O, Schleyer M, Schwartz P, Hütter JF, Spieckermann PG. Development of ischemia-induced damage in defined mitochondrial subpopulations. *J Mol Cell Cardiol* 1985;17:885–896
75. Zorzano A, Liesa M, Sebastián D, Segalés J, Palacín M. Mitochondrial fusion proteins: dual regulators of morphology and metabolism. *Semin Cell Dev Biol* 2010;21:566–574
76. Kuznetsov AV, Lassnig B, Margreiter R, Gnaiger E. Diffusion limitation of oxygen versus ADP in permeabilized muscle fibers. In *Bio-ThermoKinetics in the Post Genomic Era*. Larsson C, Pählman I-L, Gustafsson L, Eds. Göteborg, Chalmers Reproservice, 1998, p. 273–276
77. Milner DJ, Mavroidis M, Weisleder N, Capetanaki Y. Desmin cytoskeleton linked to muscle mitochondrial distribution and respiratory function. *J Cell Biol* 2000;150:1283–1298
78. Saks VA, Veksler VI, Kuznetsov AV, et al. Permeabilized cell and skinned fiber techniques in studies of mitochondrial function in vivo. *Mol Cell Biochem* 1998;184:81–100
79. Kay L, Nicolay K, Wieringa B, Saks V, Wallimann T. Direct evidence for the control of mitochondrial respiration by mitochondrial creatine kinase in oxidative muscle cells in situ. *J Biol Chem* 2000;275:6937–6944
80. Vercesi AE, Bernardes CF, Hoffmann ME, Gadelha FR, Docampo R. Digitonin permeabilization does not affect mitochondrial function and allows the determination of the mitochondrial membrane potential of *Trypanosoma cruzi* in situ. *J Biol Chem* 1991;266:14431–14434
81. Veksler VI, Kuznetsov AV, Sharov VG, Kapelko VI, Saks VA. Mitochondrial respiratory parameters in cardiac tissue: a novel method of assessment by using saponin-skinned fibers. *Biochim Biophys Acta* 1987;892:191–196
82. Gosalvez M, Garcia-Suarez S, Lopez-Alarcon L. Metabolic control of glycolysis in normal and tumor permeabilized cells. *Cancer Res* 1978;38:142–148

83. Kraunsøe R, Boushel R, Hansen CN, et al. Mitochondrial respiration in subcutaneous and visceral adipose tissue from patients with morbid obesity. *J Physiol* 2010;588:2023–2032
84. Ducluzeau PH, Priou M, Weitheimer M, et al. Dynamic regulation of mitochondrial network and oxidative functions during 3T3-L1 fat cell differentiation. *J Physiol Biochem* 2011;67:285–296
85. Woodward HE, Alsberg CL. A comparison of the effect of certain saponins on the surface tension of water with their hemolytic power. *J Pharmacol Exp Ther* 1920;16:237–245
86. Hostettmann K, Marston A. *Saponins*. Cambridge, New York, Cambridge University Press, 1995
87. Korn ED. Cell membranes: structure and synthesis. *Annu Rev Biochem* 1969;38:263–288
88. Comte J, Maisterrena B, Gautheron DC. Lipid composition and protein profiles of outer and inner membranes from pig heart mitochondria. Comparison with microsomes. *Biochim Biophys Acta* 1976;419:271–284
89. Bangham AD, Horne RW, Glauert AM, Dingle JT, Lucy JA. Action of saponin on biological cell membranes. *Nature* 1962;196:952–955
90. Launikonis BS, Stephenson DG. Effects of beta-escin and saponin on the transverse-tubular system and sarcoplasmic reticulum membranes of rat and toad skeletal muscle. *Pflugers Arch* 1999;437:955–965
91. Herland JS, Julian FJ, Stephenson DG. Halothane increases Ca<sup>2+</sup> efflux via Ca<sup>2+</sup> channels of sarcoplasmic reticulum in chemically skinned rat myocardium. *J Physiol* 1990;426:1–18
92. Launikonis BS, Stephenson DG. Effect of saponin treatment on the sarcoplasmic reticulum of rat, cane toad and crustacean (yabby) skeletal muscle. *J Physiol* 1997;504:425–437
93. Brookes PS, Yoon Y, Robotham JL, Anders MW, Sheu SS. Calcium, ATP, and ROS: a mitochondrial love-hate triangle. *Am J Physiol Cell Physiol* 2004;287:C817–C833
94. Wikström M, Casey R. The oxidation of exogenous cytochrome c by mitochondria. Resolution of a long-standing controversy. *FEBS Lett* 1985;183:293–298
95. Doran E, Halestrap AP. Cytochrome c release from isolated rat liver mitochondria can occur independently of outer-membrane rupture: possible role of contact sites. *Biochem J* 2000;348:343–350
96. Gnaiger E, Kuznetsov AV. Mitochondrial respiration at low levels of oxygen and cytochrome c. *Biochem Soc Trans* 2002;30:252–258
97. Toleikis A, Trumbeckaite S, Majiene D. Cytochrome C effect on respiration of heart mitochondria: influence of various factors. *Biosci Rep* 2005;25:387–397
98. Von Ahnen O, Waterhouse NJ, Kuwana T, Newmeyer DD, Green DR. The 'harmless' release of cytochrome c. *Cell Death Differ* 2000;7:1192–1199
99. Cogswell AM, Stevens RJ, Hood DA. Properties of skeletal muscle mitochondria isolated from subsarcolemmal and intermyofibrillar regions. *Am J Physiol* 1993;264:C383–C389
100. Matlib MA, Rouslin W, Kraft G, Berner P, Schwartz A. On the existence of two populations of mitochondria in a single organ. Respiration, calcium transport and enzyme activities. *Biochem Biophys Res Commun* 1978;84:482–488
101. Kuznetsov AV, Kunz WS, Saks V, et al. Cryopreservation of mitochondria and mitochondrial function in cardiac and skeletal muscle fibers. *Anal Biochem* 2003;319:296–303
102. Larsen S, Wright-Paradis C, Gnaiger E, Helge JW, Boushel R. Cryopreservation of human skeletal muscle impairs mitochondrial function. *Cryo Lett* 2012;33:170–176
103. Ventura-Clapier R, Vassort G. Role of myofibrillar creatine kinase in the relaxation of rigor tension in skinned cardiac muscle. *Pflugers Arch* 1985;404:157–161
104. Murphy RM. Enhanced technique to measure proteins in single segments of human skeletal muscle fibers: fiber-type dependence of AMPK- $\alpha$ 1 and - $\beta$ 1. *J Appl Physiol* 2011;110:820–825
105. Larsen S, Nielsen J, Hansen CN, et al. Biomarkers of mitochondrial content in skeletal muscle of healthy young human subjects. *J Physiol* 2012;590:3349–3360
106. Leary SC, Battersby BJ, Hansford RG, Moyes CD. Interactions between bioenergetics and mitochondrial biogenesis. *Biochim Biophys Acta* 1998;1365:522–530
107. Rodríguez-Enríquez S, Juárez O, Rodríguez-Zavala JS, Moreno-Sánchez R. Multisite control of the Crabtree effect in ascites hepatoma cells. *Eur J Biochem* 2001;268:2512–2519
108. Sachan DS, Hoppel CL. Carnitine biosynthesis. Hydroxylation of N<sup>6</sup>-trimethyl-lysine to 3-hydroxy-N<sup>6</sup>-trimethyl-lysine. *Biochem J* 1980;188:529–534
109. Gnaiger E, Kuznetsov AV, Schneeberger S, et al. Mitochondria in the cold. In *Life in the Cold*. Heldmaier G, Lingenspor M, Eds. Heidelberg, Berlin, New York, Springer, 2000, p. 431–442
110. Anderson EJ, Lustig ME, Boyle KE, et al. Mitochondrial H<sub>2</sub>O<sub>2</sub> emission and cellular redox state link excess fat intake to insulin resistance in both rodents and humans. *J Clin Invest* 2009;119:573–581
111. Fasching M, Renner-Sattler K, Gnaiger E. *Mitochondrial Respiration Medium - MiRO6*. OROBOROS MiPNet Publications, 2011
112. Gnaiger E, Kuznetsov AV, Rieger G, et al. Mitochondrial defects by intracellular calcium overload versus endothelial cold ischemia/reperfusion injury. *Transpl Int* 2000;13(Suppl. 1):S555–S557
113. Guzun R, Gonzalez-Granillo M, Karu-Varikmaa M, et al. Regulation of respiration in muscle cells in vivo by VDAC through interaction with the cytoskeleton and MtCK within Mitochondrial Interactosome. *Biochim Biophys Acta* 2012;1818:1545–1554
114. Walsh B, Tonkonogi M, Söderlund K, Hultman E, Saks V, Sahlin K. The role of phosphorylcreatine and creatine in the regulation of mitochondrial respiration in human skeletal muscle. *J Physiol* 2001;537:971–978
115. Perry CG, Kane DA, Herbst EA, et al. Mitochondrial creatine kinase activity and phosphate shuttling are acutely regulated by exercise in human skeletal muscle. *J Physiol* 2012;590:5475–5486
116. Veksler VI, Kuznetsov AV, Anfous K, et al. Muscle creatine kinase-deficient mice. II. Cardiac and skeletal muscles exhibit tissue-specific adaptation of the mitochondrial function. *J Biol Chem* 1995;270:19921–19929
117. Seppet EK, Kaambre T, Sikk P, et al. Functional complexes of mitochondria with Ca, MgATPases of myofibrils and sarcoplasmic reticulum in muscle cells. *Biochim Biophys Acta* 2001;1504:379–395
118. Chau-Berlinck JG, Monteiro LH, Navas CA, Bicudo JE. Temperature effects on energy metabolism: a dynamic system analysis. *Proc Biol Sci* 2002;269:15–19
119. Blier PU, Breton S, Desrosiers V, Lemieux H. Functional conservatism in mitochondrial evolution: insight from hybridization of arctic and brook charrs. *J Exp Zool B Mol Dev Evol* 2006;306:425–432
120. Almeida-Val VM, Buck LT, Hochachka PW. Substrate and acute temperature effects on turtle heart and liver mitochondria. *Am J Physiol* 1994;266:R858–R862
121. Ali SS, Marcondes MC, Bajova H, Dugan LL, Conti B. Metabolic depression and increased reactive oxygen species production by isolated mitochondria at moderately lower temperatures. *J Biol Chem* 2010;285:32522–32528
122. Dufour S, Rousse N, Canioni P, Diolez P. Top-down control analysis of temperature effect on oxidative phosphorylation. *Biochem J* 1996;314:743–751
123. Brown JC, Chung DJ, Belgrave KR, Staples JF. Mitochondrial metabolic suppression and reactive oxygen species production in liver and skeletal muscle of hibernating thirteen-lined ground squirrels. *Am J Physiol Regul Integr Comp Physiol* 2012;302:R15–R28
124. Anderson EJ, Yamazaki H, Neuffer PD. Induction of endogenous uncoupling protein 3 suppresses mitochondrial oxidant emission during fatty acid-supported respiration. *J Biol Chem* 2007;282:31257–31266
125. Pate E, Cooke R. The inhibition of muscle contraction by adenosine 5' (beta, gamma-imido) triphosphate and by pyrophosphate. *Biophys J* 1985;47:773–780
126. Kovács M, Tóth J, Hetényi C, Málnási-Csizmadia A, Sellers JR. Mechanism of blebbistatin inhibition of myosin II. *J Biol Chem* 2004;279:35557–35563
127. Cheung A, Dantzig JA, Hollingworth S, et al. A small-molecule inhibitor of skeletal muscle myosin II. *Nat Cell Biol* 2002;4:83–88
128. Anmann T, Eimre M, Kuznetsov AV, et al. Calcium-induced contraction of sarcomeres changes the regulation of mitochondrial respiration in permeabilized cardiac cells. *FEBS J* 2005;272:3145–3161
129. Kuznetsov AV, Guzun R, Boucher F, Bagur R, Kaambre T, Saks V. Mysterious Ca(2+)-independent muscular contraction: déjà vu. *Biochem J* 2012;445:333–336
130. Gnaiger E. Capacity of oxidative phosphorylation in human skeletal muscle: new perspectives of mitochondrial physiology. *Int J Biochem Cell Biol* 2009;41:1837–1845
131. Scandurra FM, Gnaiger E. Cell respiration under hypoxia: facts and artefacts in mitochondrial oxygen kinetics. *Adv Exp Med Biol* 2010;662:7–25
132. Gnaiger E. Oxygen conformance of cellular respiration. A perspective of mitochondrial physiology. *Adv Exp Med Biol* 2003;543:39–55
133. Boushel R, Gnaiger E, Schjerling P, Skovbro M, Kraunsøe R, Dela F. Patients with type 2 diabetes have normal mitochondrial function in skeletal muscle. *Diabetologia* 2007;50:790–796
134. Aragónés J, Schneider M, Van Geyte K, et al. Deficiency or inhibition of oxygen sensor Phd1 induces hypoxia tolerance by reprogramming basal metabolism. *Nat Genet* 2008;40:170–180
135. Boushel R, Gnaiger E, Calbet JA, et al. Muscle mitochondrial capacity exceeds maximal oxygen delivery in humans. *Mitochondrion* 2011;11:303–307

136. Chance B, Leigh JS Jr, Clark BJ, et al. Control of oxidative metabolism and oxygen delivery in human skeletal muscle: a steady-state analysis of the work/energy cost transfer function. *Proc Natl Acad Sci USA* 1985;82: 8384–8388
137. Chance B, Williams GR. Respiratory enzymes in oxidative phosphorylation. I. Kinetics of oxygen utilization. *J Biol Chem* 1955;217:383–393
138. Kemp GJ, Radda GK. Quantitative interpretation of bioenergetic data from  $^{31}\text{P}$  and  $^1\text{H}$  magnetic resonance spectroscopic studies of skeletal muscle: an analytical review. *Magn Reson Q* 1994;10:43–63
139. Chance B, Leigh JS Jr, Kent J, McCully K. Metabolic control principles and  $^{31}\text{P}$  NMR. *Fed Proc* 1986;45:2915–2920
140. Kent-Braun JA, Ng AV. Skeletal muscle oxidative capacity in young and older women and men. *J Appl Physiol* 2000;89:1072–1078
141. Lanza IR, Befroy DE, Kent-Braun JA. Age-related changes in ATP-producing pathways in human skeletal muscle in vivo. *J Appl Physiol* 2005;99:1736–1744
142. Radda GK, Bore PJ, Gadian DG, et al.  $^{31}\text{P}$  NMR examination of two patients with NADH-CoQ reductase deficiency. *Nature* 1982;295:608–609
143. Walter G, Vandenborne K, McCully KK, Leigh JS. Noninvasive measurement of phosphocreatine recovery kinetics in single human muscles. *Am J Physiol* 1997;272:C525–C534
144. Conley KE, Jubrias SA, Esselman PC. Oxidative capacity and ageing in human muscle. *J Physiol* 2000;526:203–210
145. Quistorff B, Johansen L, Sahlin K. Absence of phosphocreatine resynthesis in human calf muscle during ischaemic recovery. *Biochem J* 1993; 291:681–686
146. Crowther GJ, Kemper WF, Carey MF, Conley KE. Control of glycolysis in contracting skeletal muscle. II. Turning it off. *Am J Physiol Endocrinol Metab* 2002;282:E74–E79
147. Jubrias SA, Crowther GJ, Shankland EG, Gronka RK, Conley KE. Acidosis inhibits oxidative phosphorylation in contracting human skeletal muscle in vivo. *J Physiol* 2003;553:589–599
148. Lanza IR, Wigmore DM, Befroy DE, Kent-Braun JA. In vivo ATP production during free-flow and ischaemic muscle contractions in humans. *J Physiol* 2006;577:353–367
149. Lanza IR, Bhagra S, Nair KS, Port JD. Measurement of human skeletal muscle oxidative capacity by  $^{31}\text{P}$ -MR spectroscopy: a cross-validation with in vitro measurements. *J Magn Reson Imaging* 2011;34:1143–1150
150. Larson-Meyer DE, Newcomer BR, Hunter GR, Hetherington HP, Weinsier RL.  $^{31}\text{P}$  MRS measurement of mitochondrial function in skeletal muscle: reliability, force-level sensitivity and relation to whole body maximal oxygen uptake. *NMR Biomed* 2000;13:14–27
151. Layec G, Bringard A, Le Fur Y, et al. Reproducibility assessment of metabolic variables characterizing muscle energetics in vivo: A  $^{31}\text{P}$ -MRS study. *Magn Reson Med* 2009;62:840–854
152. McCully KK, Turner TN, Langley J, Zhao Q. The reproducibility of measurements of intramuscular magnesium concentrations and muscle oxidative capacity using  $^{31}\text{P}$  MRS. *Dyn Med* 2009;8:5
153. Larson-Meyer DE, Newcomer BR, Hunter GR, Joannisse DR, Weinsier RL, Bamman MM. Relation between in vivo and in vitro measurements of skeletal muscle oxidative metabolism. *Muscle Nerve* 2001;24:1665–1676
154. McCully KK, Fielding RA, Evans WJ, Leigh JS Jr, Posner JD. Relationships between in vivo and in vitro measurements of metabolism in young and old human calf muscles. *J Appl Physiol* 1993;75:813–819
155. Amara CE, Marcinek DJ, Shankland EG, Schenkman KA, Arakaki LS, Conley KE. Mitochondrial function in vivo: spectroscopy provides window on cellular energetics. *Methods* 2008;46:312–318
156. Argov Z, De Stefano N, Arnold DL. ADP recovery after a brief ischemic exercise in normal and diseased human muscle—a  $^{31}\text{P}$  MRS study. *NMR Biomed* 1996;9:165–172
157. Befroy DE, Shulman GI. Magnetic resonance spectroscopy studies of human metabolism. *Diabetes* 2011;60:1361–1369
158. Kemp GJ, Brindle KM. What do magnetic resonance-based measurements of Pi→ATP flux tell us about skeletal muscle metabolism? *Diabetes* 2012; 61:1927–1934
159. Befroy DE, Petersen KF, Dufour S, et al. Impaired mitochondrial substrate oxidation in muscle of insulin-resistant offspring of type 2 diabetic patients. *Diabetes* 2007;56:1376–1381
160. Kacerovsky-Bielesz G, Chmelik M, Ling C, et al. Short-term exercise training does not stimulate skeletal muscle ATP synthesis in relatives of humans with type 2 diabetes. *Diabetes* 2009;58:1333–1341
161. Laurent D, Yerby B, Deacon R, Gao J. Diet-induced modulation of mitochondrial activity in rat muscle. *Am J Physiol Endocrinol Metab* 2007;293: E1169–E1177
162. Lim EL, Hollingsworth KG, Smith FE, Thelwall PE, Taylor R. Effects of raising muscle glycogen synthesis rate on skeletal muscle ATP turnover rate in type 2 diabetes. *Am J Physiol Endocrinol Metab* 2011;301:E1155–E1162
163. Petersen KF, Befroy D, Dufour S, et al. Mitochondrial dysfunction in the elderly: possible role in insulin resistance. *Science* 2003;300:1140–1142
164. Szendroedi J, Schmid AI, Meyerspeer M, et al. Impaired mitochondrial function and insulin resistance of skeletal muscle in mitochondrial diabetes. *Diabetes Care* 2009;32:677–679
165. Jucker BM, Ren J, Dufour S, et al.  $^{13}\text{C}/^{31}\text{P}$  NMR assessment of mitochondrial energy coupling in skeletal muscle of awake fed and fasted rats. Relationship with uncoupling protein 3 expression. *J Biol Chem* 2000;275:39279–39286
166. Choi CS, Befroy DE, Codella R, et al. Paradoxical effects of increased expression of PGC-1 $\alpha$  on muscle mitochondrial function and insulin-stimulated muscle glucose metabolism. *Proc Natl Acad Sci USA* 2008;105: 19926–19931
167. Cline GW, Vidal-Puig AJ, Dufour S, Cadman KS, Lowell BB, Shulman GI. In vivo effects of uncoupling protein-3 gene disruption on mitochondrial energy metabolism. *J Biol Chem* 2001;276:20240–20244
168. Befroy DE, Falk Petersen K, Rothman DL, Shulman GI. Assessment of in vivo mitochondrial metabolism by magnetic resonance spectroscopy. *Methods Enzymol* 2009;457:373–393
169. Kemp GJ. The interpretation of abnormal  $^{31}\text{P}$  magnetic resonance saturation transfer measurements of Pi/ATP exchange in insulin-resistant skeletal muscle. *Am J Physiol Endocrinol Metab* 2008;294:E640–642; author reply E643–644
170. Gnaiger E, Méndez G, Hand SC. High phosphorylation efficiency and depression of uncoupled respiration in mitochondria under hypoxia. *Proc Natl Acad Sci USA* 2000;97:11080–11085
171. Amara CE, Shankland EG, Jubrias SA, Marcinek DJ, Kushmerick MJ, Conley KE. Mild mitochondrial uncoupling impacts cellular aging in human muscles in vivo. *Proc Natl Acad Sci USA* 2007;104:1057–1062
172. Jucker BM, Dufour S, Ren J, et al. Assessment of mitochondrial energy coupling in vivo by  $^{13}\text{C}/^{31}\text{P}$  NMR. *Proc Natl Acad Sci USA* 2000;97:6880–6884
173. Kane DA, Anderson EJ, Price JW 3rd, et al. Metformin selectively attenuates mitochondrial  $\text{H}_2\text{O}_2$  emission without affecting respiratory capacity in skeletal muscle of obese rats. *Free Radic Biol Med* 2010;49: 1082–1087